

Algebraic Displacement Correlation in Two-Dimensional Polymer Melts

J. P. Wittmer,* H. Meyer, A. Johner, T. Kreer, and J. Baschnagel

Institut Charles Sadron, 23 rue du Loess, BP 84047, 67034 Strasbourg Cedex 2, France

(Received 3 February 2010; published 15 July 2010)

Dense self-avoiding polymer chains in strictly two dimensions are compact objects with fractal contours. Using scaling arguments and molecular dynamics simulations (with negligible momentum conservation) it is shown that correlated amoebalike fluctuations of the (sub)chain contours dominate the relaxation dynamics on all scales. The incompressibility of the melt and the compactness of (sub)chains impose a scale-free constraint on the contour fluctuations. This leads to strong long range spatiotemporal correlations of the displacement field as shown, e.g., by the (negative) algebraic decay of the center-of-mass velocity correlation function $C(t) \sim -1/t^{6/5}$ with time t .

DOI: 10.1103/PhysRevLett.105.037802

PACS numbers: 61.25.H-, 47.53.+n, 61.20.Lc

Dense, essentially incompressible two-dimensional (2D) simple liquids with conserved momentum are known to exhibit strong, long-range correlations of the particle displacement field [1,2]. The coupling of displacement and momentum fields manifests itself in $d = 2$ dimensions by the slow algebraic decay of the velocity correlation function (VCF), $C(t) \equiv \langle \mathbf{v}(t) \cdot \mathbf{v}(0) \rangle \sim +1/t^{d/2} = +1/t$ with $\mathbf{v}(t)$ being the particle velocity at time t , as revealed by the seminal molecular dynamics (MD) simulations of Alder and Wainwright [1]. Interestingly, even if the momentum conservation is dropped, as justified for overdamped dense colloidal suspensions [2,3], scale-free—albeit much weaker—correlations of the displacement field are to be expected due to the incompressibility constraint [2,3]. The coupling of a tagged colloid to the collective density dipole field, created by the colloid's own displacement at $t = 0$, leads to a negative algebraic long-time decay of the VCF, $C(t) \sim -1/t^{d/2+1} = -1/t^2$ [2–4]. In this Letter, we explore another complex fluid, a 2D polymer melt, and demonstrate that the $-1/t^2$ long-time behavior of the center-of-mass VCF is preceded by another much slower algebraic decay which results from the interplay of melt incompressibility and equilibrium conformational properties.

As shown in Fig. 1, we investigate the displacement correlations in strictly 2D melts of “self-avoiding walks” without monomer overlap and chain crossing [5,6]. We remind the reader that these chains adopt compact conformations of typical size $R(N) \sim N^{1/d}$ [5–10] with fractal contours of perimeter $L(N) \sim R(N)^{d_p}$, N being the chain length and $d_p = 5/4$ the fractal line dimension [5,6]. Because of the self-similar structure of the chains, compactness and perimeter fractality repeat for subchains of arc lengths $s \leq N$ down to a few monomers [5,6,11]. Since the fractality of the (sub)chain contours precludes a finite line tension of the perimeter, there should be no activation barrier between two chain conformations and amoebalike shape fluctuations are not suppressed exponentially [5,8]. Considering a (sub)chain deformed by a thermal fluctuation dissipating the acquired energy $k_B T$ within a relaxa-

tion time $\tau(s)$ by friction at its contour, it was predicted that the relaxation time scales as [5,12]

$$\tau(s) \sim L(s)^3 \sim s^\alpha \quad \text{with} \quad \alpha = 3d_p/d = 15/8 < 2; \quad (1)$$

i.e., the dynamics should thus be slightly faster than that of Rouse-like models where $\alpha = 2$ [5,13]. We will confirm Eq. (1) numerically below. More importantly, extending [5] we demonstrate in this study by means of scaling arguments and MD simulations that the amoebalike contour fluctuations are highly correlated. As seen from the flow patterns in Fig. 1, this implies strong long range spatiotemporal correlations of the displacement field similar to those obtained for liquids with momentum conservation, although our systems are obtained by MD

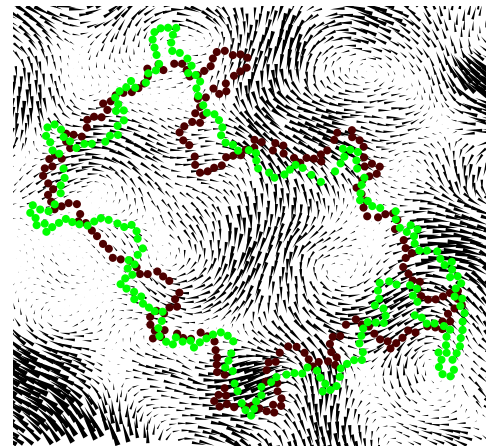


FIG. 1 (color online). Snapshot of the monomer displacement field (small arrows) in a strictly two-dimensional polymer melt of “self-avoiding walks” [5,6] as obtained by MD simulations with negligible momentum conservation. The existence of long range dynamical correlations is obvious from the observed flow pattern. The contour monomers (interacting with monomers from other chains) for one chain before and after the time interval corresponding to the displacement field are indicated by dark and light spheres, respectively.

simulations using a Langevin thermostat for which momentum conservation is irrelevant [14,15]. We will show that these long range correlations correspond for times $t \ll \tau(s)$ to an analytic decay of the VCF associated with the center of mass (c.m.) of the (sub)chains

$$C(t, s) \approx -\left(\frac{R(s)}{\tau(s)}\right)^2 \left(\frac{t}{\tau(s)}\right)^{-2+(1+\beta)/\alpha} \quad (2)$$

$$\sim -s^{-1/2} t^{-6/5} \quad (3)$$

with $\beta = 1/2$ being a second dynamical power-law exponent which, together with the exponent α , characterizes the proposed ‘‘amoeba diffusion model.’’

As in previous work on static properties [6] we represent the polymer chains by the Kremer-Grest bead-spring model [16]. Lennard-Jones units are employed in the following. We focus on monodisperse melts at temperature $T = 1$ and monomer number density $\rho = 7/8$ corresponding to 98 304 monomers in a periodic simulation box with chain lengths ranging up to $N = 1024$. The equations of motion are solved via the Velocity-Verlet algorithm using a Langevin thermostat with the standard choice for the friction constant, $\gamma = 0.5$, which leads to overdamped motion on the monomer scale [14,15].

The numerical verification of the first key element of the amoeba diffusion model, Eq. (1), from the measured relaxation times is difficult (albeit possible as shown in Fig. 4) since the exponent α is rather close to that of Rouse-like models [5]. More readily, it can be demonstrated from the functional form of various dynamic correlation functions, as the monomer mean-square displacement (MSD) $\xi^2(t) \equiv \langle u_i^2(t) \rangle_i$ presented in Fig. 2 with $u_i(t) = r_i(t) - r_i(0)$ being the displacement vector of monomer i . We note that the amoeba dynamics is characterized by one time scale $\tau(N) \sim N^\alpha$ and the reduced MSD $\xi^2(t)/R^2(N)$ must be a function of $t/\tau(N)$. Since the MSD is chain

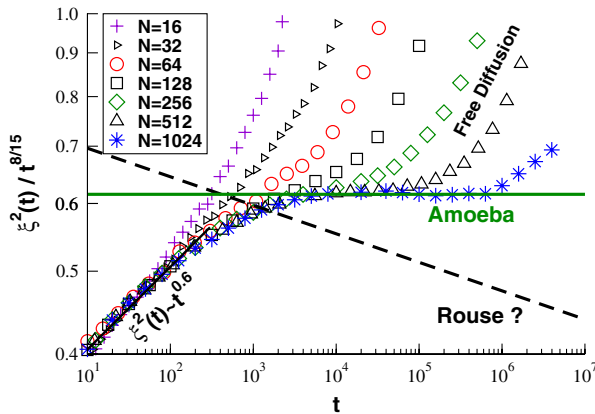


FIG. 2 (color online). Monomer MSD $\xi^2(t)$ for chains of length N as indicated. The vertical axis is rescaled with the prediction $\xi^2(t) \sim t^{8/15}$ of the amoeba diffusion model. The transient short-time regime is fitted to a phenomenological power law. For large times ($t \gg 10^3$) the data approach with increasing N the predicted horizontal line.

length independent for short times $t \ll \tau(N)$, it follows that

$$\xi^2(t) \approx R^2(N)[t/\tau(N)]^{1/\alpha} \sim N^0 t^{1/\alpha}. \quad (4)$$

The vertical axis of Fig. 2 is rescaled by the amoeba prediction to show that the data approach this limit for large N while the Rouse model (dashed line) is inconsistent with our data. Note that our longest chain, $N = 1024$, fits the amoeba model (horizontal line) over two decades. This confirms the first exponent of the amoeba diffusion model; we now turn to discuss the second exponent β .

Because of the compactness of the chains a tagged monomer moving over a distance $\xi(t)$ must drag along $g(t) \sim \xi^2(t)$ monomers it is connected to. The monomer displacement field is thus at least correlated locally on the scale $\xi(t)$ of this ‘‘dynamical blob.’’ That the displacement field is in fact correlated on much larger scales, as suggested by Fig. 1, is addressed in Fig. 3 which displays the temporal correlations of the c.m. displacement vector $u_{cm}(t) = \sum_i u_i(t)/s$ of (sub)chains. Focusing first on the MSD $\xi_{cm}^2(t) \equiv \langle u_{cm}^2(t) \rangle$ (main panel) we rescaled the measured MSD in terms of the dynamical blob and plot $\xi_{cm}(t)/\xi(t)$ as a function of the rescaled time $x = \xi(t)/R(s)$. This allows us to collapse all data onto one master curve. As one expects, $\xi_{cm}(t)/\xi(t) \rightarrow 1$ for $x \gg 1$, i.e., $t \gg \tau(s)$, when the (sub)chain has moved *en bloc* over a distance comparable to its own size. For smaller times we obtain over nearly three decades a power law,

$$\xi_{cm}(t)/\xi(t) \approx [\xi(t)/R(s)]^\beta \quad \text{with } \beta \approx 1/2 \quad (5)$$

(bold line) [17]. Clearly, if there were no long range

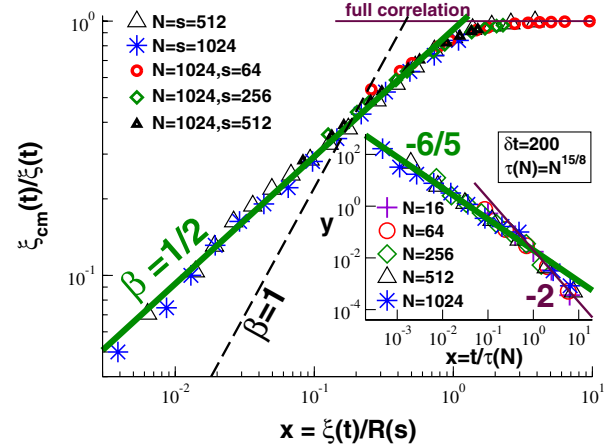


FIG. 3 (color online). c.m. displacement for chains of length N and subchains of length s for $N = 1024$ as indicated. Main panel: Scaling of the ratio $\xi_{cm}(t)/\xi(t)$ as a function of $x = \xi(t)/R(s)$ with $R(s)$ being the typical size of the (sub)chain. Demonstrating long range correlations between dynamical blobs of size $\xi(t)$ a power-law exponent $\beta = 1/2$ is observed for $x \leq 1$. Inset: Collapse of the rescaled VCF $y = -C(t, N)/[R(N)/\tau(N)]^2$ vs reduced time $x = t/\tau(N)$ for different N and $\delta t = 200$. The bold line indicates the exponent $-6/5$ predicted by Eq. (3) for $x \ll 1$.

correlations between the dynamical blobs, $\xi_{\text{cm}}^2(t)$ would be given by $\xi^2(t)$ times a factor $1/(s/g(t))^2$ due to the normalization of the c.m. times the number of uncorrelated dynamical blobs, $s/g(t)$. This would imply $\xi_{\text{cm}}(t) \approx \xi^2(t)/R(s)$, i.e., $\beta = 1$ (dashed line), at variance to our data. That an exponent $\beta < 1$ is observed is expected from the flow pattern shown in Fig. 1; we still need to explain why the exponent should actually become $\beta = 1/2$. Because of the incompressibility of the melt and the compactness of the (sub)chains the c.m. can only change by means of contour fluctuations. These fluctuations must be correlated since the overall (sub)chain surface is constant for all s and a subsegment of $g(t)$ monomers added at one point of the contour corresponds to the same mass taken off the contour at a distance $R(s)$. The MSD $\xi_{\text{cm}}^2(t)$ is thus given by $R^2(s)$ times the normalization factor $1/[s/g(t)]^2$ times the number $R(s)/\xi(t)$ of independent blobs one can create and annihilate on the contour of the (sub)chain [18]. This leads to $\xi_{\text{cm}}^2(t) \approx \xi^2(t)/R(s)$, i.e., $\beta = 1/2$ as observed. The existence of long range correlations between dynamical blobs due to the constant surface constraint is the central result of this Letter.

Using Eq. (4) it follows from Eq. (5) that as a function of time one expects

$$\xi_{\text{cm}}^2(t) \sim s^{-\beta} t^{(1+\beta)/\alpha} \sim s^{-1/2} t^{4/5} \quad (6)$$

for $t \ll \tau(s)$ and $1 \ll s \leq N$: i.e., the stochastic forces acting on the (sub)chain c.m. are strongly colored. The VCF $C(t, s) \equiv \langle \mathbf{v}_{\text{cm}}(t) \cdot \mathbf{v}_{\text{cm}}(0) \rangle \sim \partial_t^2 \xi_{\text{cm}}^2(t)$ [2] of the (sub)chains allows an independent numerical verification of the claimed power laws with respect to s and t . We remind the reader that the VCF would vanish exponentially if only white forces were present [2,17]. As a corollary of Eqs. (1), (4), and (5) one obtains instead the analytic decay of the VCF announced in Eqs. (2) and (3). Note that the scaling result has been reformulated in Eq. (2) in terms of the natural scaling variables, the velocity scale $R(s)/\tau(s)$ and the reduced time $x = t/\tau(s)$. These predictions are tested numerically in the inset of Fig. 3 where the “velocity” $\mathbf{v}_{\text{cm}}(t) \equiv \mathbf{u}_{\text{cm}}(\delta t)/\delta t$ of a (sub)chain at time t has been obtained from its c.m. displacement $\mathbf{u}_{\text{cm}}(\delta t)$ for a small time increment $\delta t \ll t$. Focusing on chain displacements ($s = N$) the rescaled VCF $y = -C(t, N)/[R(N)/\tau(N)]^2$ is plotted as a function of the reduced time x assuming $\tau(N) \equiv N^{15/8}$. This leads to a perfect data collapse for all N demonstrating that y is indeed a scaling function of x [17]. The exponent $-6/5$ predicted for small reduced times $x \ll 1$ nicely fits the data over three decades in time. The decay of the VCF becomes much more rapid for $x \gg 1$ with an exponent -2 (thin line) fitting the data, i.e., $C(t, N) \sim -N/t^2$. For large times, the chains thus move as expected for overdamped two-dimensional colloids [2,4].

Interestingly, the amoeba diffusion model can, in principle, be verified experimentally by means of the dynamical intrachain structure factor $F(q, t)$ with q being the wave

vector [13]. How $F(q, t)$ may be analyzed is addressed in Fig. 4 for $N = 1024$. The inset on the left presents the relaxation time τ_q defined by $F(q, t = \tau_q)/F(q) = 1/e$. The vertical axis is rescaled by the Rouse prediction $\tau_q \sim 1/q^4$ [13]. The scaling of τ_q is a direct consequence of Eq. (1),

$$\tau_q \sim s^\alpha \sim R(s)^{\alpha/\nu} \sim 1/q^{\alpha/\nu} = 1/q^{15/4}. \quad (7)$$

As indicated by the bold line our data increase as $\tau_q q^4 \approx q^{1/4}$ over 1 order of magnitude for $q > 1/R(N)$, confirming thus again Eq. (1). The main panel and the inset on the right present the reduced dynamical structure factor $y = 1 - F(q, t)/F(q)$ for different reduced wave vectors $Q = R(N)q$. In the Guinier limit (right inset) $F(q, t)$ probes the overall chain motion and the horizontal scaling variable is $x = \xi_{\text{cm}}(t)q$ using the c.m. displacement $\xi_{\text{cm}}(t)$ at time t discussed above. For small x , $F(q, t)$ can be expanded [13], yielding $y = x^2/4$ in agreement with the data. The main panel presents wave vectors $Q > 1$ which probe the monomer dynamics within the chain. A perfect data collapse is obtained if y is traced vs $x = \xi(t)q$ with $\xi(t)$ being the monomer displacement. For small times we find a power law $y \approx x^\delta$ with $\delta = 3$ rather than the exponent $\delta = 4$ of the Rouse model. This exponent δ can be understood by matching the small- Q and the large- Q regimes by choosing a wave vector $q = 1/R(N)$ which implies $[\xi(t)/R(N)]^\delta \approx [\xi_{\text{cm}}(t)/R(N)]^2$. Comparing this with Eq. (5) yields $\delta = 2 + 2\beta = 3$. The experimental observation of a power-law slope of the reduced dynamical structure factor with $\delta \approx 3$ would thus confirm long range correlations characterized by an exponent $\beta \approx 1/2$.

In summary, using scaling arguments and MD simulations we investigated the equilibrium dynamics of strictly

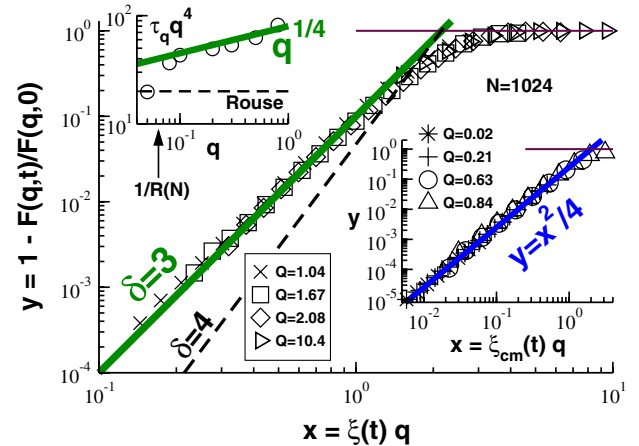


FIG. 4 (color online). Dynamical structure factor $F(q, t)$ for $N = 1024$ with $Q = R(N)q$ as indicated. The relaxation time τ_q is presented in the left inset. The main panel and the right inset show the short-time behavior of the reduced dynamic structure factor $y = 1 - F(q, t)/F(q)$ for large and small Q , respectively. The dashed lines correspond to the Rouse model, the bold lines to the amoeba diffusion model.

2D polymer melts without chain overlap [5,6]. Following [5] we argued that the chain relaxation is dominated by amoebalike fluctuations of the fractal contours of the compact (sub)chains. These fluctuations may be described in terms of two exponents $\alpha = 15/8$ and $\beta = 1/2$ characterizing, respectively, the relaxation time of the (sub)chains (as predicted by [5]) and the long range correlations of the monomer displacement field of a tagged (sub)chain, Eq. (5). The latter correlations arise due to the compactness of the chains and the incompressibility of the melt implying a scale-free constraint on the c.m. displacements as manifested by the observed algebraic decay of the associated VCF, Eq. (3). The exponent β may be verified experimentally by means of the dynamical intrachain structure factor $F(q, t)$ predicted to scale as $1 - F(q, t)/F(q) \sim q^3$ for short times and $q \gg 1/R(N)$.

Systems of dense polymer layers are of experimental relevance [9,10,19,20]. It should thus be stressed that several modeling assumptions made above may readily be relaxed: (i) Our predictions are not restricted to polymer melts but should also hold in semidilute solutions [7] provided that the chains are sufficiently long. Assuming a density independent effective local mobility, standard density crossover scaling [7] suggests that the self-diffusion constant, $D_s(\rho, N) \sim \rho^{1/4}N^{-7/8}$, increases strongly with density rather than to remain constant as implied by the Rouse model. This scaling may allow us to interpret recent experimental data [19]. (ii) We have assumed sufficient frictional contact of the monomers to the supporting surface to suppress long range correlations due to momentum conservation. This boundary condition is indeed well justified experimentally for polymers adsorbed on rough solid surfaces [10,19] or phospholipid bilayers [9]. Since for perfectly smooth surfaces or fluid-air interfaces [20] this may not hold, it should be emphasized that even for friction constants $\gamma \ll 0.5$, where standard 2D hydrodynamics kicks in, the exponents α and β are numerically found to hold for internal modes computed in the c.m. frame of the chains. (iii) Our discussion has focused on strictly 2D self-avoiding walks without chain crossings. In practice, so-called “self-avoiding trails” with finite chain crossing probability [5] may be more relevant being readily realized experimentally by ultrathin polymer films where the 2D projections of chain loops can cross. Preliminary numerical results suggest, however, that if crossings are allowed with a penalty of order $5k_B T$ both static and dynamic properties remain well described (at least for chains with $N \leq 1024$) by the infinite penalty limit we have focused on.

We thank A. N. Semenov and S. P. Obukhov for useful discussions and acknowledge financial support by the Deutsche Forschungsgemeinschaft (Grant No. KR 2854/1-1) as well as a generous grant of computer time by GENCI-IDRIS (Grant No. i2009091467).

- *joachim.wittmer@ics-cnrs.unistra.fr
- [1] B. J. Alder and T. E. Wainwright, *Phys. Rev. A* **1**, 18 (1970).
 - [2] J. K. G. Dhont, *An Introduction to Dynamics of Colloids* (Elsevier, Amsterdam, 1996).
 - [3] M. Fuchs and K. Kroy, *J. Phys. Condens. Matter* **14**, 9223 (2002).
 - [4] M. H. J. Hagen, I. Pagonabarraga, C. P. Lowe, and D. Frenkel, *Phys. Rev. Lett.* **78**, 3785 (1997).
 - [5] A. N. Semenov and A. Johner, *Eur. Phys. J. E* **12**, 469 (2003).
 - [6] H. Meyer, T. Kreer, M. Aichele, A. Cavallo, A. Johner, J. Baschnagel, and J. Wittmer, *Phys. Rev. E* **79**, 050802(R) (2009).
 - [7] P. G. de Gennes, *Scaling Concepts in Polymer Physics* (Cornell University Press, Ithaca, New York, 1979).
 - [8] I. Carmesin and K. Kremer, *J. Phys. (Paris)* **51**, 915 (1990).
 - [9] B. Maier and J. O. Rädler, *Phys. Rev. Lett.* **82**, 1911 (1999).
 - [10] F. C. Sun, A. V. Dobrynin, D. S. Shirvanyants, H. I. Lee, K. Matyjaszewski, G. J. Rubinstein, M. Rubinstein, and S. S. Sheiko, *Phys. Rev. Lett.* **99**, 137801 (2007).
 - [11] Taking advantage of the fractal and hierarchical structure of static and dynamical properties we often do not distinguish between properties on the scale of a segment of length s and the overall chain of length $s = N$.
 - [12] As argued in [5] the dissipation rate $\mathcal{D}(s)$ due to a subchain of s monomers must be proportional to the number of contour monomers $L(s)$ times the friction force acting on each monomer times the velocity of the monomer. Summing up the contributions from all subchains yields $\mathcal{D}(N)\tau(N) \sim L(N)^3/\tau(N)$ for the total energy dissipated by the chain. Being equal to the thermal energy $k_B T$, this implies Eq. (1) for $s = N$.
 - [13] M. Doi and S. F. Edwards, *The Theory of Polymer Dynamics* (Clarendon Press, Oxford, 1986).
 - [14] B. Dünweg, *J. Chem. Phys.* **99**, 6977 (1993).
 - [15] Our molecular dynamics simulations are supported by dynamic Monte Carlo (MC) simulations, not included here for clarity of presentation. Displacement fields similar to that shown in Fig. 1 have been obtained, although there is no “momentum conservation” in MC.
 - [16] K. Kremer and G. Grest, *J. Chem. Phys.* **92**, 5057 (1990).
 - [17] Equations (5) and (6) hold numerically only for sufficiently large chains with $N \gg 128$ where the additional white noise contribution (essentially generated by the thermostat) becomes irrelevant. Importantly, the VCF $C(t, s) \sim \partial_t^2 \xi_{cm}^2(t)$ focusing on the colored noise scales for all $N \geq 16$ according to Eq. (2).
 - [18] We assume here that the projected Euclidean contour of order $R(s) \sim s^{1/2}$ sets the number of uncorrelated surface modes and not the fractal perimeter length $L(s) \sim s^{5/8}$. Note that the numerical difference between both assumptions is too small to be tested in our simulations.
 - [19] J. Zhao and S. Granick, *Macromolecules* **40**, 1243 (2007).
 - [20] S. Srivastava and J. K. Basu, *J. Chem. Phys.* **130**, 224907 (2009).